Histol Histopathol (2026) 41: 1065-1079

Histology and Histopathology
From Cell Biology to Tissue Engineering

ORIGINAL ARTICLE Open Access

Downregulation of PDCD10 mitigates the malignant biological behavior and increases the sensitivity of esophageal squamous cell carcinoma cells to radiotherapy by inhibiting the PI3K/AKT pathway

Junkai Xu, Qisong Chen and Qing Gao

Department of Radiotherapy, The Affiliated Hospital of Putian University, Putian City, Fujian Province, China

Summary. The intensification of radiotherapy is an effective way to improve the therapeutic efficacy of radiation-sensitive malignancies such as esophageal cancer (EC). Esophageal squamous cell carcinoma (ESCC) accounts for 85% of all EC cases worldwide, with a relatively higher incidence and mortality in East Asia. In this study, we explored the functions and mechanisms of programmed cell death 10 (PDCD10) in the malignancy and radiotherapy sensitivity of ESCC cells. We observed that PDCD10 is highly expressed in ESCC tissues and is correlated with a poor prognosis in patients with ESCC. PDCD10 downregulation suppressed ESCC cell proliferation, migration, and invasion but promoted apoptosis. In addition, it enhanced ionizing radiation (IR)-induced ESCC cell damage, whereas PDCD10 overexpression had the opposite effect. Mechanistically, PDCD10 increased the phosphorylation of phosphatidylinositol 3-kinase (PI3K) and protein kinase B (AKT) in ESCC cell lines. The administration of LY294002, a PI3K inhibitor, significantly inhibited the oncogenic functions of PDCD10, leading to an increase in IR-induced cell damage. These findings establish PDCD10 as a critical intrinsic regulator of the sensitivity of ESCC cells to IR through the modulation of the PI3K/AKT pathway.

Keywords: PDCD10, Esophageal squamous cell carcinoma, Radiotherapy, PI3K/AKT pathway

Corresponding Author: Junkai Xu, Department of Radiotherapy, The Affiliated Hospital of Putian University, No. 999 Dongzhen East Road, Gongchen Street, Licheng District, Putian City 351100, Fujian Province, China. e-mail: junkai_xu@163.com

www.hh.um.es. DOI: 10.14670/HH-25-010

Introduction

Esophageal cancer (EC) is an aggressive malignancy with the seventh-highest incidence and sixth-highest mortality worldwide (Sung, 2021; Qi et al., 2024). Globally, EC affects mainly men, and the incidence and mortality in men are 2-3 times greater than in women (Sung et al., 2021). The incidence and mortality of EC gradually increase with age and increase sharply from the age of 50 (Qi et al., 2024). East Asia accounts for nearly half of new EC cases and EC-related deaths worldwide. Among them, China alone accounts for 43.8% of new cases of EC and 42.1% of deaths worldwide. EC ranks third in cancer-related deaths in 2024 in China (Wu et al., 2024). Esophageal squamous cell carcinoma (ESCC) accounts for 85% of all EC cases worldwide (Morgan et al., 2022). Owing to the lack of early symptoms of ESCC, most patients with ESCC are diagnosed at an advanced stage, resulting in a poor overall prognosis with a five-year survival rate of <20% (Zhao et al., 2024). Surgical resection, chemotherapy, and radiotherapy are conventional treatments for ESCC but face great challenges in the clinic (Tong et al., 2024). For example, ESCC cells easily metastasize, and surgery can hardly eliminate the tumor entirely (Zhang et al., 2022). Severe liver and kidney injury, gastrointestinal diseases, bleeding, and other side effects often accompany chemotherapy. The long-term use of chemotherapy drugs inevitably leads to drug resistance (Romani, 2022). Radiotherapy can kill cancer cells by ionizing radiation (IR). Nevertheless, it can cause unnecessary radiation damage to healthy tissues around the irradiated area and trigger an adaptive response in the tumor, resulting in radioresistance (Farhood et al., 2020). These limitations have become difficult problems that need to be overcome in the treatment of cancer. It is important to explore the potential targets and pathogenesis of cancer to identify new treatment strategies for patients with ESCC.

During the progression of ESCC, changes in gene and protein expression are accompanied by the direct regulation of cancer progression. For example, butyrophilin 3A1 (BTN3A1) is overexpressed in ESCC, which promotes the malignant progression and radioresistance of ESCC cells by activating the UNC-51-like kinase 1 (ULK1) pathway and increasing the level of autophagy in cancer cells (Yang et al., 2022). Phosphatidylinositol 3-kinase (PI3K) is a lipid kinase that can propagate intracellular signaling cascades and regulate multiple cellular processes (Liu et al., 2020). Following the stimulation of extracellular signals, such as growth factors, hormones, or cytokines, PI3K becomes phosphorylated. Protein kinase B (Akt), a serine/threonine kinase, is a pivotal downstream molecule of PI3K (Glaviano et al., 2023). Activated PI3K promotes the phosphorylation of Akt by activating 3-phosphoinositide-dependent kinase 1 (PDK1) and mammalian target of rapamycin complex 2 (mTORC2) to fully activate Akt and form a signal transduction network (Saxton and Sabatini, 2017). PI3K/Akt signaling pathway activation is closely related to enhanced cancer cell proliferation and metastasis (Spangle et al., 2017; Ediriweera et al., 2019; Fattahi et al., 2020; Miricescu et al., 2020; Xu et al., 2021a,b; Liu et al., 2022a; Luo et al., 2022; Lyu et al., 2025). The PI3K/Akt axis can affect the radioresistance of cancers. For example, Friend leukemia integration 1 transcription factor (FLI1) activates the PI3K/Akt signaling pathway by upregulating tyrosine kinase with immunoglobulin-like and EGF-like domains 1 (TIE1), thereby affecting the radiotherapy sensitivity of nasopharyngeal carcinoma (NPC) (Chen et al., 2023a).

Programmed cell death 10 (PDCD10) is a member of the *PDCD* gene family, contains seven coding exons and three noncoding exons, and encodes a 25 kDa protein (Liu et al., 2022b). *PDCD10* has been widely studied in cerebral cavernous malformation (CCM) and is one of the three causative genes of CCM (Valentino et al., 2020). Recently, several studies have reported that PDCD10 promotes various types of cancer. For example, PDCD10 can promote epithelial-mesenchymal transition (EMT) and metastasis of liver cancer cells (Sun et al., 2021). In breast cancer, PDCD10 overexpression or Rho-associated coiled coil kinase (ROCK) inhibition can reverse the contractile phenotype induced by tripartite motif-containing 59 (TRIM59) deletion, thereby accelerating cell migration, invasion, and tumor formation (Tan et al., 2018). We are more interested in whether PDCD10 plays a role in digestive system cancers. In pancreatic cancer (PDAC), PDCD10 promotes tumor cell survival and proliferation by specifically enhancing the mitogenic function of transforming growth factor beta (TGF-β) (Zhou et al., 2024). Therefore, PDCD10 may also play an essential role in the progression of ESCC.

In this study, we found that PDCD10 was highly expressed in ESCC tissues compared with adjacent normal tissues. Further analysis revealed that higher PDCD10 expression predicts poorer prognosis in ESCC patients. Therefore, we conducted experiments to determine the role of PDCD10 in the malignant progression of ESCC cells both *in vitro* and *in vivo*, and the radiotherapy sensitivity of ESCC cells was also determined. PDCD10 upregulation activated the PI3K/Akt signaling pathway, suggesting that the PI3K/Akt axis plays a role in PDCD10-mediated oncogenic functions. Taken together, the results of this study show that targeting PDCD10 may provide new opportunities for treating ESCC.

Materials and methods

Cell culture

The human ESCC cell lines, including Eca-109 (Cat. No. TCHu69) and KYSE-150 (Cat. No. TCHu236), were purchased from the cell bank of the Chinese Academy of Sciences (Shanghai, China). These two cell lines were cultured in RPMI 1640 medium supplemented with 10% fetal bovine serum (FBS, Cat. No. 40130ES50; Yeasen, Shanghai, China) and 1% penicillin/streptomycin (Cat. No. 60162ES76; Yeasen, Shanghai, China). An incubator with a constant temperature of 37°C, 5% CO_2, and saturated humidity was used for cell culture. ESCC cells were treated with the PI3K inhibitor LY294002 (0.2 μM, HY-10108, MCE, NJ, US) (Xu et al., 2021a,b). For cell counting, the cells were stained with Trypan blue via a Trypan blue staining cell viability assay kit (Cat. No. C0011, Beyotime, Shanghai, China). The number of cells was counted via an automatic cell counter (C100-Pro, RWD, Shenzhen, China).

Quantitative RT-PCR (qRT-PCR)

Total RNA was extracted from the EC cell lines with TRIzol (Cat. No. 15596026CN, Invitrogen™), using ultraviolet spectrophotometry to examine RNA content and agarose gel electrophoresis (AGE) to detect RNA integrity. The reverse transcription of total RNA into cDNA was carried out via the BeyoRT™ II cDNA First Chain Synthesis Kit (Cat. No. D7168S; Beyotime, Shanghai, China). The cDNA was used as a template for PCR amplification via a BeyoFast™ SYBR Green qPCR Mix (D7260, Beyotime, Shanghai, China). The internal reference of *PDCD10* was *GAPDH*, and the relative expression level was calculated via the $2^{-\Delta\Delta Ct}$ method (Maren et al., 2023). The sequences of the primers used were as follows: PDCD10: forward: 5′- GCCCCCTCTA TGCAGTCATGTA-3′, reverse: 5′-AGCCTTGATGAA AGCGGCTC-3′; GAPDH: forward: 5′-GGAGCGAGAT CCCTCCAAAAT-3′, reverse: 5′- GGCTGTCATAC TTCTCATGG-3′.

Western blot

The RIPA lysis buffer (Cat. No. R0010, Beyotime,

Shanghai, China), Eca-109 and KYSE-150 cells were lysed and maintained on ice for 15 min. Total protein was extracted via centrifugation, and a BCA protein concentration assay kit (Cat. No. PC0020, Beyotime, Shanghai, China) was used to determine the protein concentration. The total protein was separated via sodium dodecyl sulfate-polyacrylamide gel electrophoresis (SDS-PAGE) and then transferred to a polyvinylidene fluoride (PVDF) membrane (Cat. No. YA1701, Solarbio, Beijing, China). Following protein blocking, the membranes were incubated overnight at 4°C with primary antibodies against anti-PDCD10 polyclonal antibody (#K006814P, 1:1000, Solarbio, Beijing, China), anti-GAPDH polyclonal antibody (#K110496P, 1:2000, Solarbio, Beijing, China), anti-p-PI3K (#ab278545, Abcam, Waltham, MA, USA), anti-PI3K (#ab151549, Abcam, Waltham, MA, USA), anti-p-Akt (#ab38449, Abcam, Waltham, MA, USA), and anti-Akt (#ab8805, Abcam, Waltham, MA, USA). The membranes were washed 3-5 times with 1x tris buffered saline with Tween-20 (TBST) buffer to remove unbound primary antibodies and then incubated with the secondary antibody goat anti-rabbit IgG HRP (#SE134, 1:200, Solarbio, Beijing, China) at room temperature for 1 hour. After the membranes were washed with 1x TBST buffer, the protein bands were exposed via the use of an enhanced chemiluminescence (ECL) Western Blotting Detection Kit (Cat. No. SW2040/SW2030, Solarbio, Beijing, China). The protein signals were developed on X-films. Densitometry was performed via ImageJ (v1.8.0., NIH, Bethesda, Maryland, USA). GAPDH was used as an internal control. The relative protein expression was calculated as the fold change in the control group (vector group or sh-NC group) (Mahmood and Yang, 2012).

Cell counting kit-8 (CCK8) assay

Eca-109 and KYSE-150 cells were seeded in 96-well plates. Each well contained approximately 5000 cells. Following incubation of different durations, CCK-8 solution (10 µl) (Cat. No. CA1210, Solarbio, Beijing, China). The plates were incubated at 37°C for 2 hours. A microplate reader (A51119500C, Thermo Fisher Scientific Inc., Waltham, USA) was used to detect the absorbance (450 nm) (Chen et al., 2023b).

EdU staining assay

The cells were seeded in 24-well plates. Each well contained 1×10^5 cells. The cells were incubated in the incubator for 24h. A Beyoclick™ EdU-488 cell proliferation detection kit (Cat. No. C0071S, Beyotime, Shanghai, China) was used to detect cell proliferation. EdU working solution (20 µM) was preheated at 37°C and mixed with culture medium at a 1:1 ratio, after which the cells were cocultured for 2h. The cells were subsequently fixed with 4% paraformaldehyde (Cat. No. P0099, Beyotime, Shanghai, China) for 15 min. The nucleus was stained with 2-(4-amidinophenyl)-6-indolecarbamidine dihydrochloride (DAPI, Cat. No. C1006, Beyotime, Shanghai, China). After washing with 1x phosphate-buffered saline (PBS) twice, the cells were observed and counted via a fluorescence microscope (EVOS Flauto, Life Technologies, USA). ImageJ software was used to determine the percentage of EdU-positive cells (Zhang et al., 2024).

Colony-forming assay

Approximately 1000 Eca-109 and KYSE-150 cells were seeded in six-well plates, which were subsequently incubated with 5% CO_2 for two weeks at 37°C. The cells were fixed with 4% paraformaldehyde for 30 min. The cells were stained with crystal violet staining solution (Cat. No. C8470, Beyotime, Shanghai, China). A colony was defined as consisting of at least 50 cells under a light microscope (Olympus BX51TF; Olympus Corporation, Tokyo, Japan). The number of colonies in each well was counted (Franken et al., 2006).

Transwell assay

The Matrigel® matrix (Cat. No. #354480; Corning, NY, USA) was liquefied at 4°C overnight and then diluted with medium at a ratio of 1:6. A total of 50 µl of diluted Matrigel was added to the upper compartment to coat the membrane, which was then dried after 4h of incubation. Eca-109 and KYSE-150 cells were diluted to 1×10^6 cells/ml. The top compartment contained 100 µl of cell suspension, while 600 µl of medium containing 10% FBS was added to the bottom compartment. The cells were cultivated for approximately 24h in a 5% CO_2 incubator at 37°C. After three rinses with 1x PBS, the invading cells were fixed in 95% ethanol for 5 min, followed by 0.5% crystal violet staining for 10 min. After rinsing with 1x PBS, a cotton swab was used to gently wash noninvaded cells, and the cells under the membrane were observed via a microscope (Olympus BX51TF; Olympus Corporation, Tokyo, Japan) (Yueyang et al., 2023).

Radiation

Eca-109 and KYSE-150 cells were collected and exposed to different IR doses (2Gy, 4Gy, 6Gy, 8Gy, 10Gy) via a cabinet X-ray irradiator (RS2000, Rad Source Technologies, Suwanee, GA) (Yang et al., 2022). After that, Eca-109 and KYSE-150 cells were seeded into 96-well plates (each well contained 1×10^4 cells). Twenty-four hours later, 10 µL of CCK-8 solution (CA1210, Solarbio, Beijing, China) was added to each well. The cells were incubated at 37°C for 48 or 96h. A microplate reader (A51119500C, Thermo Fisher Scientific Inc., Waltham, USA) was used to detect the absorbance (450 nm). The percentage of cell viability

was calculated by comparing the irradiated and nonirradiated groups (0 Gy) and was used to create survival curves.

Flow cytometry

Eca-109 and KYSE-150 cells were collected and resuspended in 1x PBS. Approximately 5×10^5 cells from each group were incubated with 5 μL of Annexin V-FITC and 10 μL of PI staining solution (Cat. No. HY-K1073, MCE, NJ, USA) and then incubated at 4°C for 30 min in the dark. A flow cytometer (Cat. No. A24858, Thermo Fisher Scientific Inc., Waltham, USA) was used to analyze apoptosis (Yueyang et al., 2023).

GO and KEGG analysis

The online tool LinkedOmics (https://www.linkedomics.org/login.php) was used to identify expression patterns similar to those of *PDCD10* in EC. Pearson correlation coefficients were used to identify genes positively and negatively associated with *PDCD10*. Gene function annotation and enrichment pathway analysis were conducted via DAVID (https://davidbioinformatics.nih.gov/tools.jsp) (Sherman et al., 2024). The top 500 genes that were significantly associated with *PDCD10* in EC were included. The Gene Ontology (GO) analysis included three items: molecular function, cellular component, and biological process. Kyoto Encyclopaedia of Genes and Genomes (KEGG) functional enrichment analysis was subsequently conducted to explore the signaling pathways associated with *PDCD10*.

Animal experiments

Eca-109 cells were transfected with PDCD10-OE or sh-PDCD10. The cells with stable PDCD10 overexpression or downregulation were resuspended in 1x PBS, and the cell concentration was adjusted to 5×10^6 cells/ml. The upper right flank of male BALB/c nude mice (six weeks old; Beijing Sibeifu Biotechnology, Beijing, China) was subcutaneously injected with 100 μL of cell suspension to establish the tumor xenograft model. Fourteen days later, the tumor width (W), length (L), and height (H) were measured every four days, and the tumor volume was calculated as $W\times L\times H/2$. For anesthesia, sodium pentobarbital was prepared as a 3% sterile saline solution and administered via intraperitoneal injection (30 mg/kg body weight). Animal experiments were conducted according to the Guidelines for the Care and Use of Laboratory Animals and approved by the Ethics Committee of the Affiliated Hospital of Putian University (Approval number: 20230814). All procedures adhered to the ethical standards stated in the Declaration of Helsinki and complied with the ARRIVE guidelines. (Teng et al., 2024)

Hematoxylin-eosin (HE) staining and immunohistochemistry (IHC)

The tumor tissues were fixed with 4% paraformaldehyde for 24h and embedded in paraffin. Five-micron-thick sections were prepared. A HE staining kit (Cat. No. G1120, Solarbio, Beijing, China) was used to observe histopathological changes in the tumor tissues. The sections were placed in antigen retrieval solution (Cat. No. P0085, Beyotime, Shanghai, China) and heated for 15 min. The sections were naturally cooled to room temperature and washed three times with 1x PBS for 5 min each. The sections were blocked with a blocking solution (Cat. No. P0100A, Beyotime, Shanghai, China) for 10 min at room temperature. Next, the sections were incubated overnight at 4°Cwith an anti-PDCD10 (1:500, ab180706, Abcam, Waltham, MA, USA) antibody or anti-Ki67 antibody (1:500, ab15580, Abcam, Waltham, MA, USA). The next day, the sections were washed with 1x PBS three times for 5 min each. Then, goat anti-rabbit IgG horseradish peroxidase (HRP) (#se134, 1:200, Solarbio, Beijing, China) was added, and the samples were incubated in the dark at room temperature for 1h. After washing with 1x PBS, the DAB reagent (Cat. No. P0202, Beyotime, Shanghai, China) was used to stain the sections for 5 min at 24°C. Next, hematoxylin staining was performed for 2 min at 24°C. Subsequent observations of histomorphological alterations were carried out, and images were captured via a light microscope (Olympus BX51TF; Olympus Corporation, Tokyo, Japan). The IHC scores were determined according to a previous study (Gao et al., 2024). To detect p-PI3K and p-AKT expression, the sections were incubated with anti-phospho-Akt (Ser473) (1:300, #4060, Cell Signaling Technology, Inc., Massachusetts, USA) or phospho-PI3 kinase p55-Y199 rabbit mAb (#AP1463, 1:200, ABclonal, Wuhan, China). ABflo® 647-conjugated goat anti-rabbit IgG (H+L) (AS060, 1:200, ABclonal, Wuhan, China) was used as the secondary antibody. The nuclei were stained with DAPI solution (Cat. No. C1006, Beyotime, Shanghai, China). P-PI3K and p-AKT expression in the tissues was observed and quantified via a fluorescence microscope (EVOS Flauto, Life Technologies, USA).

Data analysis

GraphPad Prism 8.10 (GraphPad Software, La Jolla, CA, USA) was used for data analysis and visualization. Comparisons among the different groups were analyzed by one-way analysis of variance, followed by Student's t-test. $p<0.05$ was considered to indicate statistical significance.

Results

The expressions of PDCDs in EC

The expression of 15 PDCD family members in EC

and normal tissues was analyzed via the ENCORI Pancancer Analysis Platform, and the original data were integrated from the TCGA project. The data revealed that several PDCDs, including PDCD1LG2, PDCD2, PDCD2L, PDCD5, PDCD5P1, PDCD6, PDCD7, PDCD10, and PDCD11, are highly expressed in EC tissues ($p<0.05$). However, PDCD4 was expressed at lower levels in EC tissues ($p<0.05$, Table 1). Next, we analyzed the associations between PDCD family members and the overall survival of patients with EC. Higher PDCD2 and PDCD11 levels were associated with worse overall survival in EC patients ($p<0.05$, Table 1).

Knockdown of PDCD10 repressed the malignant behavior of ESCC cells

To investigate the function of PDCD10 in ESCC, we established a cell model with PDCD10 knockdown. The mRNA and protein levels after PDCD10 knockdown were detected, and the data revealed that sh-PDCD10#1 and #2 achieved 60% and 80% PDCD10 knockdown, respectively (Fig. 1A-C). CCK8 was used to detect the survival rate of ESCC cells. The viability of ESCC cells in the sh-PDCD10 group was reduced by 50% (vs. the sh-NC group, Fig. 1D,E). EdU staining and colony formation assays were performed to test cell proliferation (Fig. 1F-I). The EdU-positive rate was 56% in Eca-109 cells and 68% in KYSE-150 cells in the sh-NC group, which was reduced to 12% and 39% in Eca-109 cells and 42% and 43% in KYSE-150 cells following PDCD10 knockdown (Fig. 1F,G). The number of colonic cells in the sh-NC group was 129 (Eca-150) and 154 (KYSE-150) and was significantly reduced to 81 and 54 (Eca-150), 43 and 66 (KYSE-150) (Fig. 1H,I). Transwell assays revealed that the number of migrating and invading Eca-109 and KYSE-150 cells decreased by approximately 50% to 70% after PDCD10 knockdown (Fig. 1J-L). The apoptosis of EC cells was detected via flow cytometry. The results revealed that the proportion of apoptotic ESCC cells in the PDCD10-knockdown group (about 16% and 25% in Eca-109 cells and 21% and 17% in KYSE-150 cells) was greater than that in the sh-NC group (about 7% in Eca-109 cells and 6% in

Table 1. Expression of PDCD family members in EC and normal tissues.

Genes	Cancer num	Normal num	Cancer exp	Normal exp	Fold change	*p*-value	False discovery rate
PDCD1	162	11	1.13	0.61	1.85	0.079	0.27
PDCD1LG2	162	11	1.38	0.62	2.21	0.021	0.1
PDCD2	162	11	6.85	5.42	1.26	0.042	0.17
PDCD2L	162	11	5.14	2.32	2.22	9.50E-06	0.0002
PDCD4	162	11	15.17	35.13	0.43	4.20E-07	1.50E-05
PDCD5	162	11	19.82	9.15	2.17	5.20E-07	1.80E-05
PDCD5P1	162	11	0.49	0.24	2.04	0.0094	0.055
PDCD5P2	162	11	0.16	0.13	1.18	0.26	0.57
PDCD6	162	11	9.26	5	1.85	3.10E-06	7.80E-05
PDCD6IP	162	11	21.05	22.01	0.96	0.7	0.9
PDCD6IPP1	162	11	0.25	0.34	0.74	0.081	0.27
PDCD6IPP2	162	11	0.15	0.18	0.85	0.6	0.85
PDCD7	162	11	6.64	5.25	1.26	0.011	0.062
PDCD10	162	11	17.47	8.85	1.97	4.90E-08	2.40E-06
PDCD11	162	11	11.23	7.09	1.58	5.00E-05	0.00079

Table 2. Associations of PDCD family members with the overall survival of EC patients.

Genes	Esophageal adenocarcinoma			Esophageal squamous cell carcinoma		
	Cancer num	HR	*p*-value	Cancer num	Hazard ratio	*p*-value
PDCD1	80	1.62 (0.85-3.08)	0.140	81	2.17 (0.92-5.12)	0.070
PDCD1LG2	80	0.57 (0.25-1.3)	0.180	81	1.46 (0.57-3.71)	0.430
PDCD2	80	2.66 (1.4-5.07)	0.002	81	0.71 (0.31-1.59)	0.400
PDCD2L	80	1.95 (0.89-4.28)	0.090	81	0.48 (0.18-1.29)	0.140
PDCD4	80	0.66 (0.33-1.3)	0.220	81	2.01 (0.8-5.06)	0.130
PDCD5	80	1.86 (0.97-3.58)	0.059	81	0.44 (0.2-0.97)	0.036
PDCD6	80	1.52 (0.73-3.17)	0.260	81	2.18 (0.93-5.13)	0.067
PDCD6IP	80	1.52 (0.75-3.11)	0.240	81	1.54 (0.52-4.55)	0.440
PDCD6IPP2	80	0.57 (0.28-1.12)	0.099	81	1.45 (0.64-3.29)	0.380
PDCD7	80	1.52 (0.8-2.9)	0.190	81	0.51 (0.21-1.25)	0.140
PDCD10	80	1.75 (0.92-3.31)	0.083	81	1.98 (0.85-4.58)	0.110
PDCD11	80	1.96 (1.01-3.77)	0.041	81	0.6 (0.23-1.53)	0.280

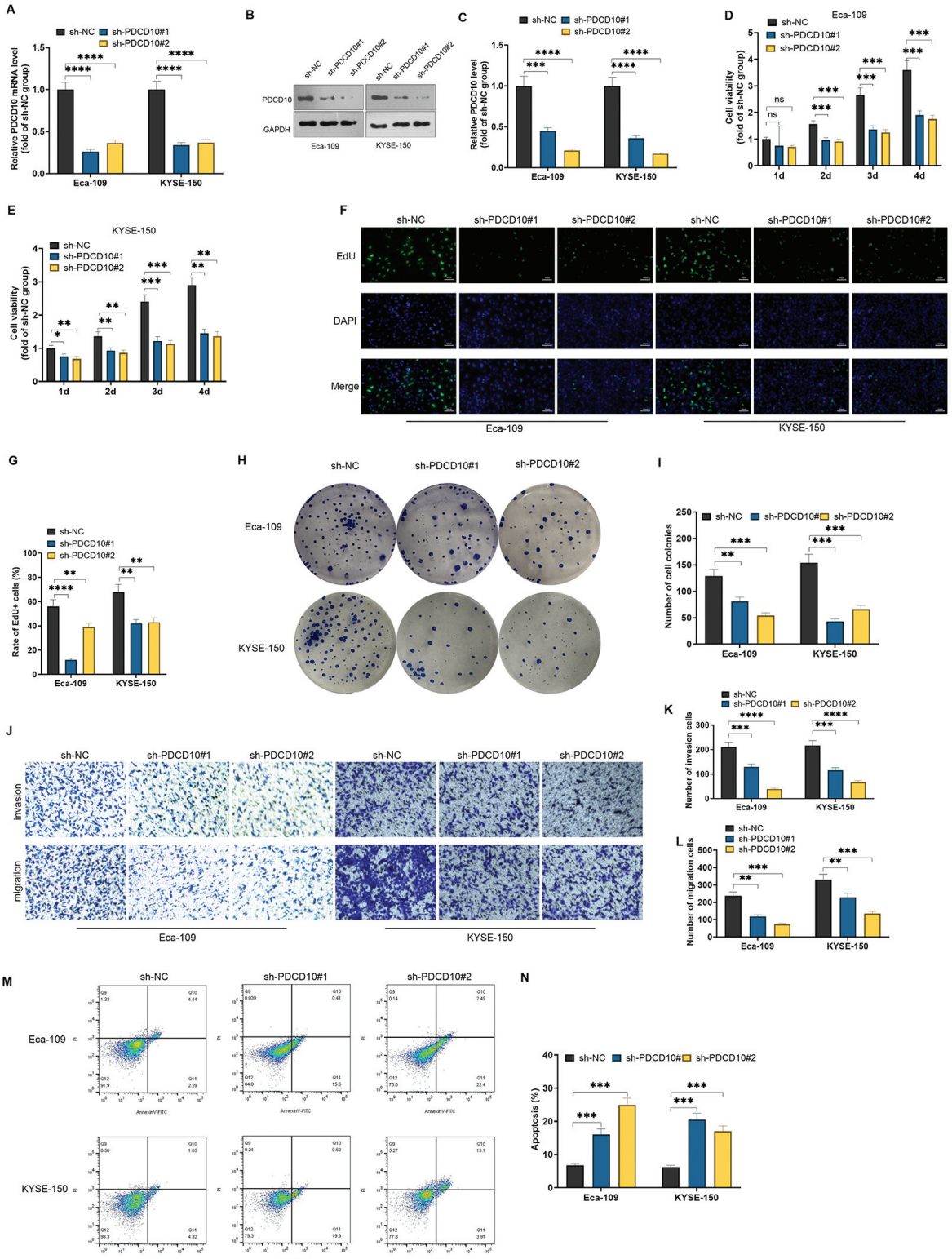

Fig. 1. Functions of PDCD10 downregulation in mediating proliferation, migration, invasion, and apoptosis. Two human ESCC cell lines, Eca-109 and KYSE-150, were transfected with sh-NC or sh-PDCD10. **A-C.** RT-PCR was used to detect the mRNA level of *PDCD10*, and western blotting was used to detect the protein level of PDCD10. **D, E.** A CCK8 assay was used to detect cell viability. **F, G.** EdU staining was used to detect cell proliferation. The percentage of EdU-positive cells was calculated. **H, I.** A colony formation assay was used to test the colony-forming ability of the cells. The number of cell colonies was calculated. **J-L.** Transwell assays were used to evaluate cell migration and invasion abilities. **M, N.** Flow cytometry was used to detect apoptosis. N=3. **p<0.01, ***p<0.001, ****p<0.0001. Scale bars: 50 μm.

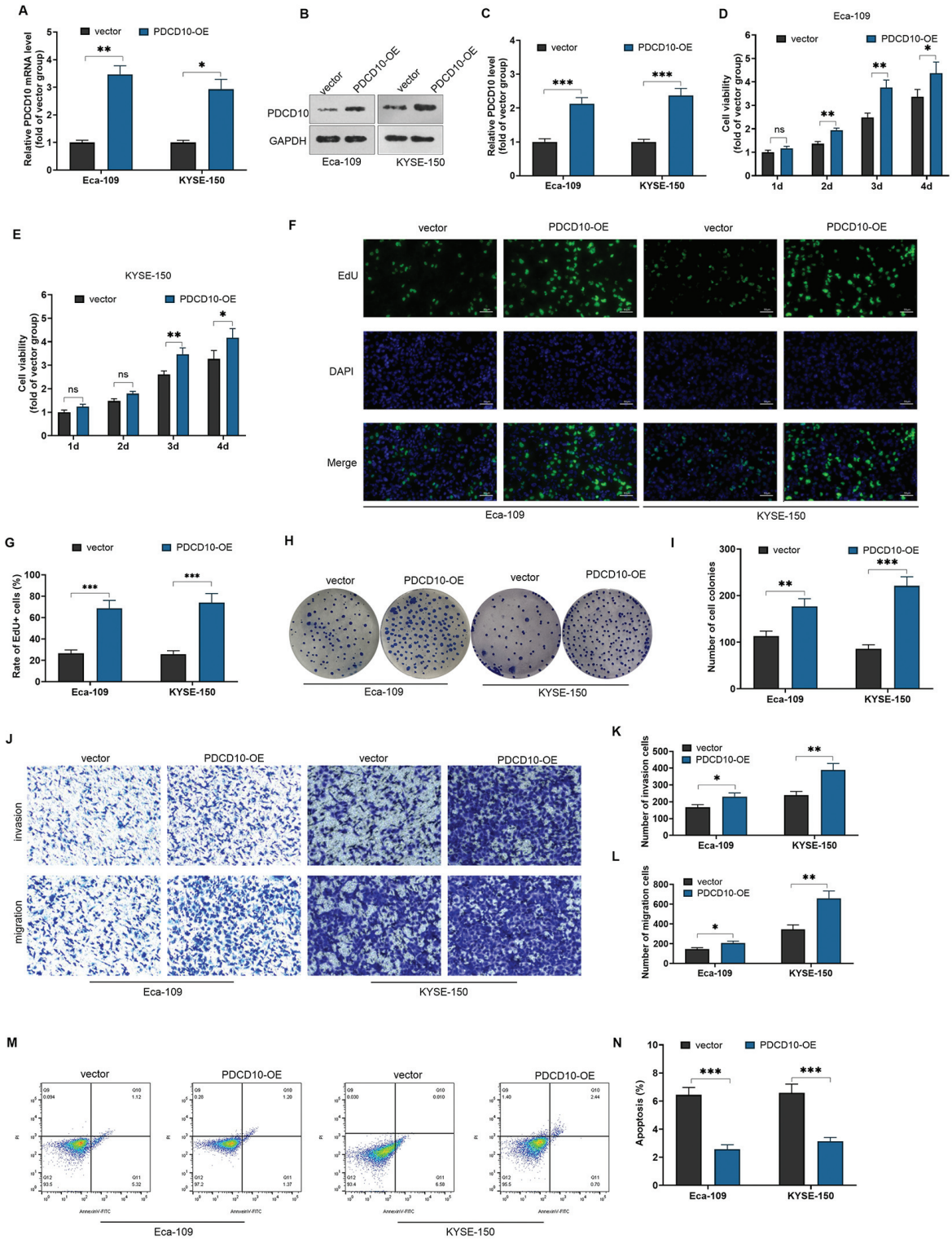

Fig. 2. Functions of PDCD10 overexpression in mediating proliferation, migration, invasion, and apoptosis. Two human ESCC cell lines, Eca-109 and KYSE-150, were transfected with a vector or PDCD10-overexpression plasmid (PDCD10-OE). **A-C.** RT-PCR was used to detect the mRNA level of *PDCD10*, and western blotting was used to detect the protein level of PDCD10. **D, E.** A CCK8 assay was used to measure cell viability. **F, G.** EdU staining was utilized to detect cell proliferation. The percentage of EdU-positive cells was calculated. Scale bar = 50 μm. **H, I.** A colony formation assay was carried out to test the colony-forming ability of the cells. The number of cell colonies was counted. **J-L.** Transwell assays were conducted to evaluate the migration and invasion abilities of the cells. **M, N.** Flow cytometry was used to detect apoptosis. N=3. ns: not significant, *p>0.05, **p<0.01, ***p<0.001, ****p<0.0001.

KYSE-150 cells) (Fig. 1M,N).

PDCD10 overexpression led to enhanced malignant behavior of ESCC cells

A PDCD10 overexpression model was constructed in ESCC cell lines (Eca-109 and KYSE-150). RT-PCR and western blotting confirmed the overexpression of PDCD10, which was 2.13-fold (Eca-109) and 2.37-fold (KYSE-150) greater than that in the vector group (Fig. 2A-C). The results of the CCK8 assay revealed that, compared with the vector control, the overexpression of PDCD10 increased the viability of ESCC cells by 0.3-fold (Eca-109) and 0.27-fold (KYSE-150) (Fig. 2D,E). The results of EdU staining and colony formation assays revealed that PDCD10 overexpression significantly enhanced the proliferation and colony formation abilities of EC cells (Fig. 2F-I). The percentage of EdU-positive cells increased from about 27% to 69% (Eca-109) and from about 26% to 74% (KYSE-150) (Fig. 1F,G). The number of colonic cells in the vector group was 113 (Eca-150) and 86 (KYSE-150), and significantly increased to 177 (Eca-150) and 221 (KYSE-150) (p<0.05, Fig. 2H,I). Transwell assays demonstrated that overexpressing PDCD10 promoted the migratory and invasive abilities of ESCC cells (Fig. 2J-L). Flow cytometry revealed that the proportion of apoptotic ESCC cells in the PDCD10-overexpressing group (about 3% of Eca-109 cells and 3% of KYSE-150 cells) was lower than that in the vector group (about 6% of Eca-109

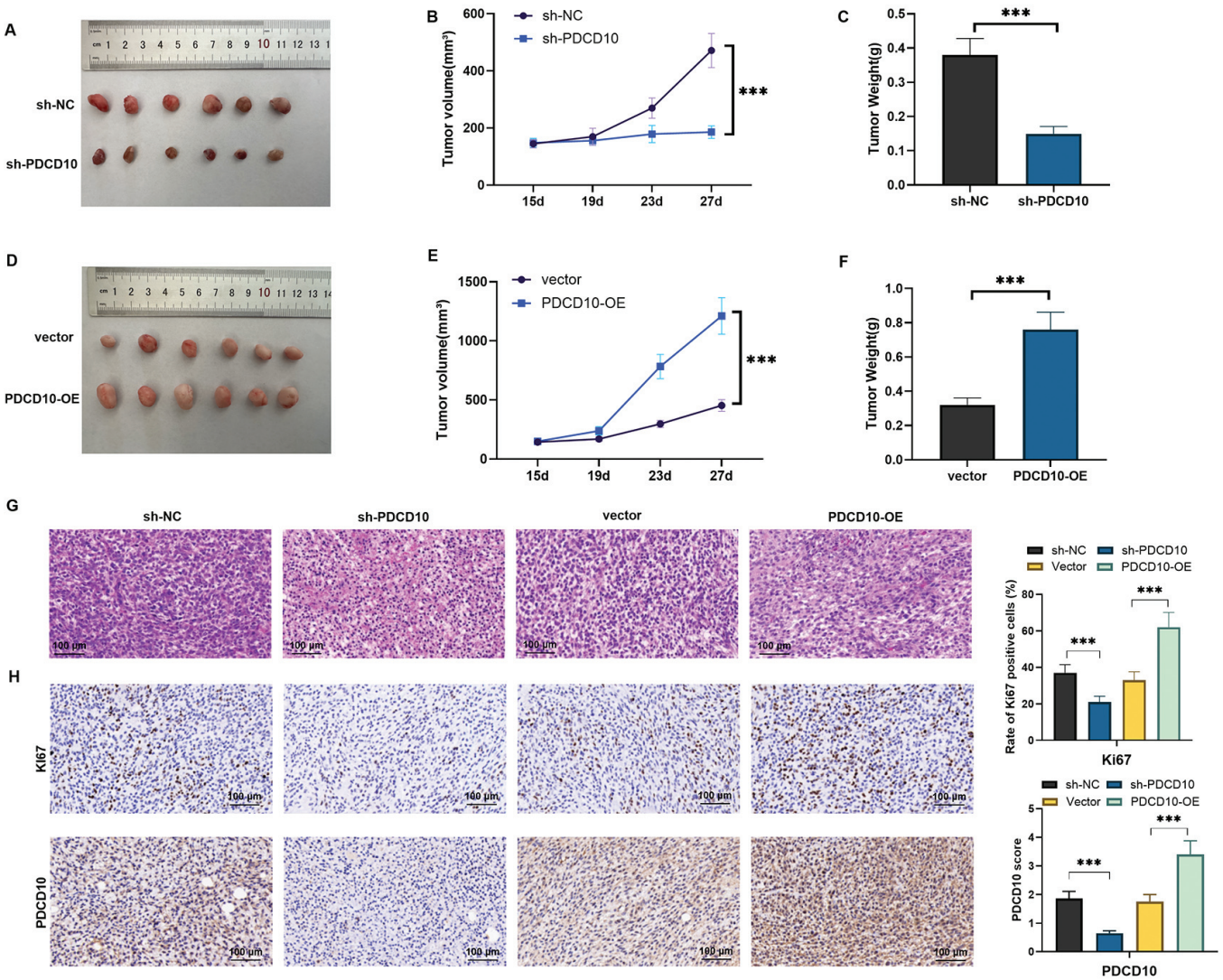

Fig. 3. Effects of PDCD10 on tumor growth. **A-C.** Images, growth curves, and weights of xenograft tumors with PDCD10 overexpression. **D-F.** Images, growth curves, and weights of xenograft tumors in which PDCD10 was knocked down. **G.** HE staining showing the pathological changes in the tumor tissues. **H-J.** IHC detection shows the expression of Ki67 and PDCD10 in tumor tissues. N=6. ns: not significant, *p>0.05, *p<0.05, **p<0.01, ***p<0.001, ****p<0.0001. Scale bars: 50 μm.

cells and about 7% of KYSE-150 cells; Fig. 2M,N).

PDCD10 promotes ESCC cell growth in vivo

To investigate the effect of PDCD10 on tumor growth *in vivo*, a xenograft tumor model was constructed in nude mice. The results revealed that the size, volume, and weight of the tumors in the sh-PDCD10 group were significantly smaller than those in the sh-NC group ($p<0.001$, Fig. 3A-C), whereas the opposite results were observed in the PDCD10-OE group (Fig. 3D-F). The results of HE staining revealed that, compared with those in the vector group, the number of blood vessels in the tumor tissue increased when PDCD10 was overexpressed (Fig. 3H). We detected the proliferation marker Ki-67 in tumor tissues. The percentage of Ki-67-positive cells was significantly decreased when PDCD10 was knocked down (37% in the sh-PDCD10 group and 21% in the sh-NC group), and the opposite effect was observed when PDCD10 was overexpressed (62% in the PDCD10-OE group and 33% in the vector group) (Fig. 3H). Moreover, the protein expression of PDCD10 was analyzed via IHC. Compared with the sh-NC group (IHC score=1.86), PDCD10 expression in the sh-PDCD10 group (IHC score=0.65) was significantly lower, and the PDCD10 level in the PDCD10-overexpressing group (IHC score=3.4) was greater than in the vector group (IHC score=1.70) (Fig. 3H).

PDCD10 knockdown enhances the radiosensitivity of ESCC cells

To investigate the effect of PDCD10 on the radiosensitivity of EC cells, we applied IR to ESCC cells and used a CCK8 assay to determine cell viability at 48 and 96h. The results revealed that the viability of Eca-109 and KYSE-150 cells decreased with increasing IR dose. When the IR dose was 10 Gy, the cell viability was 0.54-fold greater than that of the control group in Eca-109 cells, and 0.57-fold greater than that of the control group in KYSE-150 cells. PDCD10 knockdown further inhibited cell viability compared with that of the sh-NC group (the cell viability was approximately 0.35-fold greater than that of the control group) (Fig. 4A-D). However, Eca-109 and KYSE-150 cells with PDCD10 overexpression presented increased cell viability ($p<0.05$, vs. the vector group, Fig. 4E-H). These findings indicate that PDCD10 downregulation enhances the radiosensitivity of ESCC cells.

Potential mechanisms of PDCD10 in EC

The online tool LinkedOmics (https://www.linkedomics.org/login.php) was used to identify expression patterns similar to those of *PDCD10* in EC. A volcano plot of the Pearson correlation coefficients revealed genes that were positively or negatively associated with *PDCD10* (Fig. 5A). The top 50 genes with positive or negative associations are shown in a heatmap (Fig. 5B,C). The results of the GO enrichment analysis are shown in Fig. 5D. The results revealed that these genes were enriched in mediating cell migration. Moreover, the enriched KEGG pathways included breast cancer, basal cell carcinoma, hepatocellular carcinoma, gastric cancer, and the mTOR signaling pathway (Fig. 5E). PIK3CA, a vital member of the PI3K/AKT pathway, is included in those pathways. We also detected a positive correlation between PIK3CA and PDCD10 in

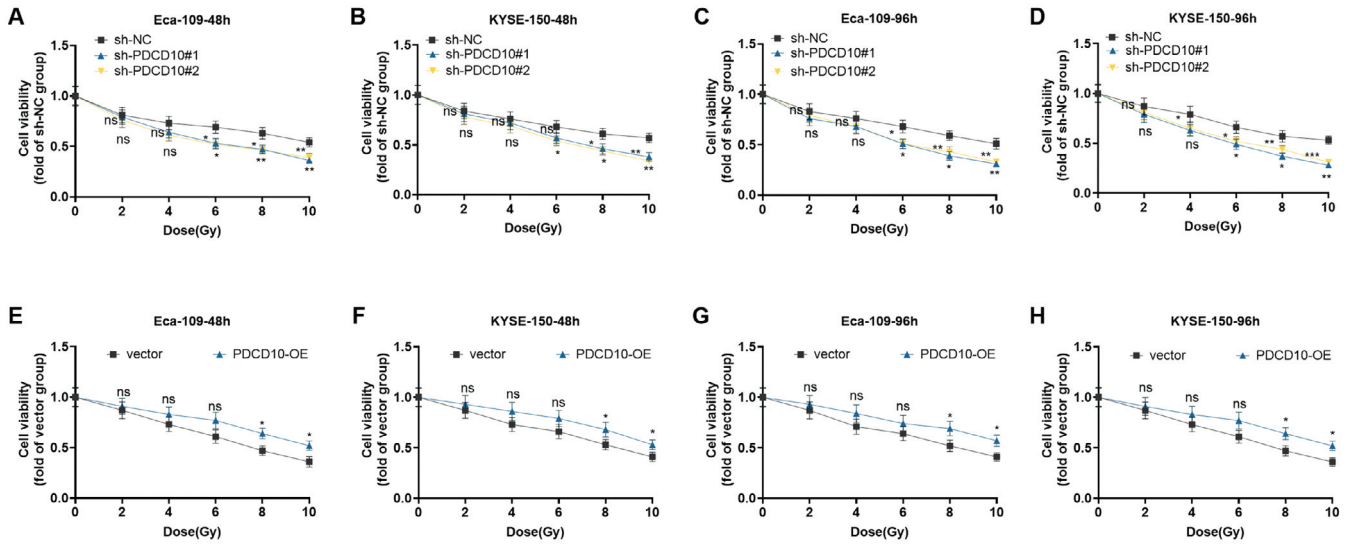

Fig. 4. The effect of PDCD10 on the radiosensitivity of ESCC cells. **A-D.** A CCK8 assay was performed at 48h and 96h to evaluate the viability of PDCD10-knockdown cells after radiation exposure (0, 2, 4, 6, 8, or 10 Gy). **E-H.** A CCK8 assay was performed at 48h and 96 h to evaluate the viability of PDCD10-overexpressing cells after radiation exposure (0, 2, 4, 6, 8, or 10 Gy). N=3. ns: not significant, $p>0.05$, *$p<0.05$, **$p<0.01$, and ***$p<0.001$.

EC (Pearson correlation coefficient=0.5141, p=8.423e-14) (Fig. 5F).

PDCD10 promotes the malignancy of ESCC cells via the PI3K/AKT pathway

We evaluated the phosphorylation of PI3K and AKT expression in Eca-109 and KYSE-150 cells with selective PDCD10 regulation. Western blotting revealed that the levels of phosphorylated PI3K and AKT in the sh-PDCD10 group were significantly decreased (p<0.05 vs. the sh-NC group, Fig. 6A-E), whereas the levels of phosphorylated PI3K and AKT were increased when PDCD10 was overexpressed (p<0.001 vs. the vector group, Fig. 6F-J). We performed immunofluorescence to detect the expression of p-PI3K and p-AKT in tumor tissues. These data confirmed that PDCD10 down-regulation attenuated the activation of the PI3K/AKT pathway. PDCD10 overexpression promoted the phosphorylation of PI3K and AKT (Fig. 6K,L). To elucidate whether PDCD10 promotes the proliferation, migration, and invasion of ESCC cells by activating the PI3K/AKT signaling pathway, we treated Eca-109 cells with the PI3K inhibitor LY294002 (0.2 μM). A colony formation assay and EdU staining were subsequently conducted. The number of colonies in the PDCD10-OE group was 196, which decreased to 132 after LY294002 treatment (p<0.01, Fig. 6M,N). The percentage of EdU-positive cells was reduced from about 56% to 36% after LY294002 treatment (p<0.05, Fig. 6O,P), revealing that the administration of the PI3K inhibitor could partially eliminate the proliferation of Eca-109 cells induced by PDCD10 overexpression. Transwell assays revealed that the inhibition of PI3K significantly weakened the migration and invasion abilities of Eca-109 cells induced by PDCD10 overexpression (p<0.05, Fig. 6Q-S).

Inhibiting the PI3K/AKT pathway enhances the radiosensitivity of ESCC cells overexpressing PDCD10

To investigate the effect of the PI3K/AKT pathway on the radiosensitivity of ESCC cells overexpressing PDCD10, we treated PDCD10-overexpressing Eca-109 and KYSE-150 cells with the PI3K inhibitor LY294002 and then subjected them to IR. The cell viability at 48 and 96 h was detected via the CCK8 assay. Compared

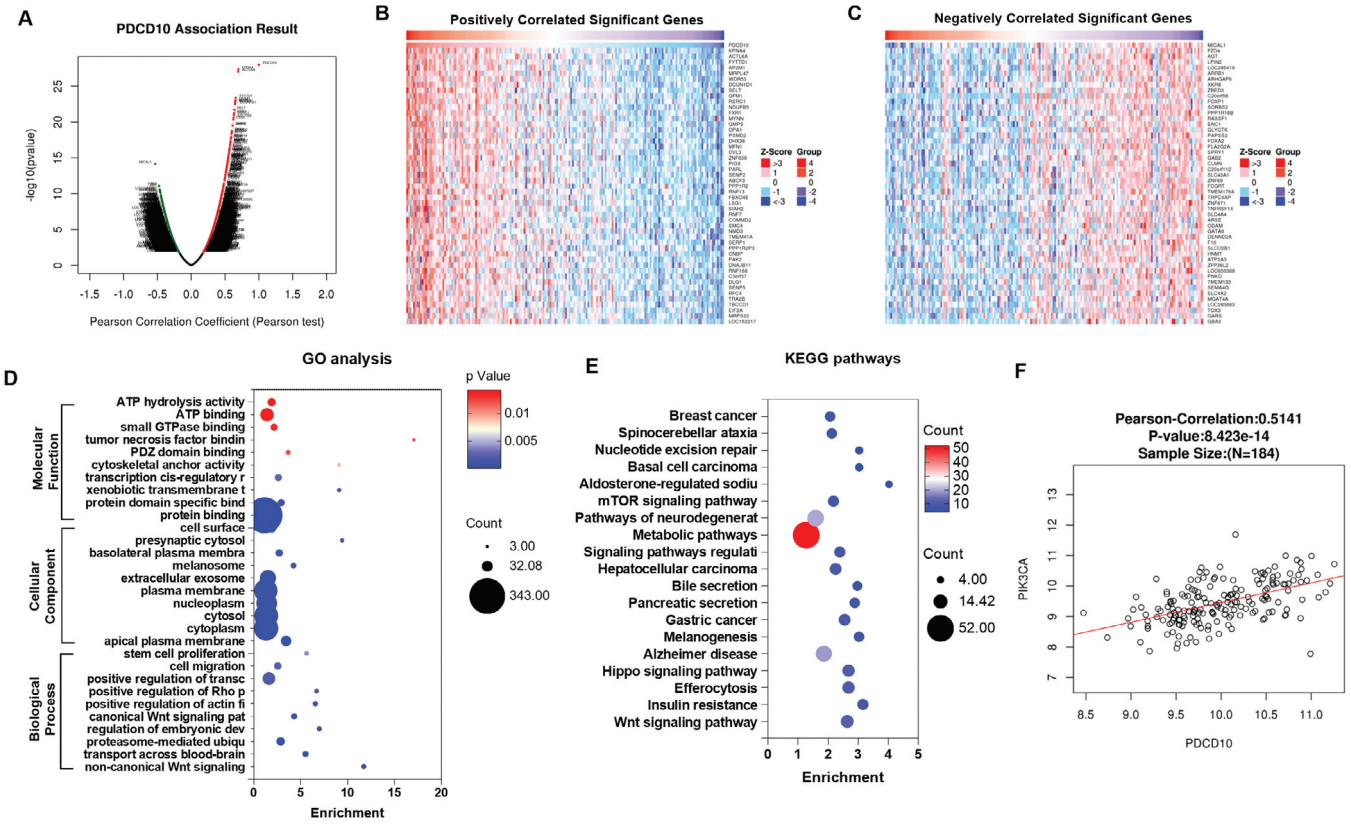

Fig. 5. Mechanistic analysis of PDCD10 in EC. **A.** A gene expression pattern similar to that of *PDCD10* in EC was analyzed via the online tool LinkedOmics (https://www.linkedomics.org/login.php). The volcano plot shows the genes positively or negatively associated with *PDCD10*. **B, C.** The top 50 genes with a positive or a negative association with *PDCD10* are shown in a heatmap. **D, E.** Gene function annotation and enrichment pathway analysis via DAVID (https://davidbioinformatics.nih.gov/tools.jsp). **F.** Scatter plot of PIK3CA and PDCD10 expression in EC (Pearson correlation coefficient=0.5141, p=8.423e-14).

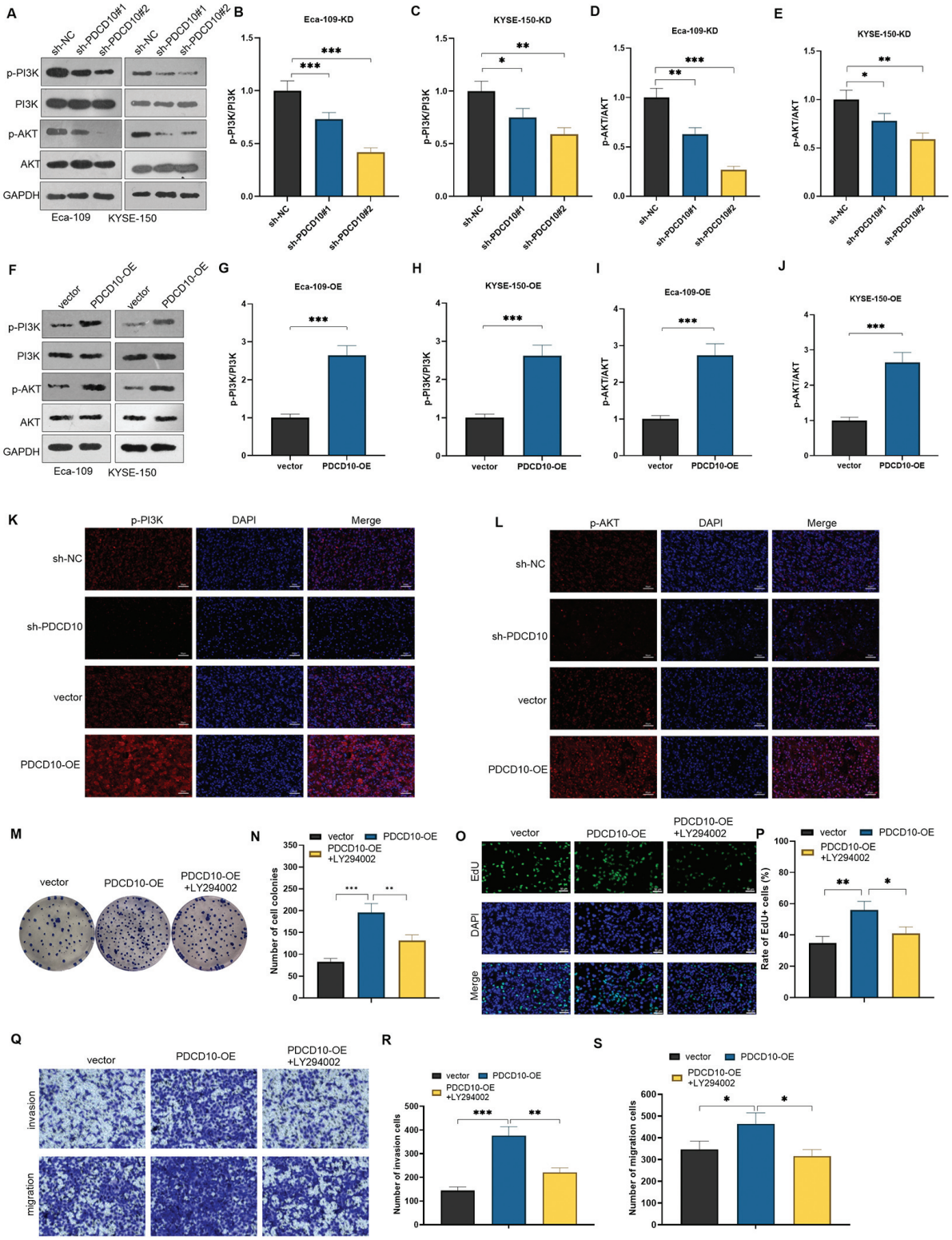

Fig. 6. Effects of PDCD10 on the PI3K/AKT pathway. **A-J.** Western blot analysis of the total and phosphorylated levels of PI3K/AKT in esophageal cancer cells with PDCD10 overexpression or knockdown. **K, L.** Representative fluorescence images of p-PI3K and p-AKT in tumor tissues. Eca-109 cells overexpressing PDCD10 were treated with the PI3K inhibitor LY294002 (0.2 μM). **M, N.** A colony formation assay was used to test the colony-forming ability of the cells. The number of cell colonies was calculated. **O, P.** EdU staining was used to detect cell proliferation. The percentage of EdU-positive cells was calculated. **Q-S.** Transwell assays were used to evaluate cell migration and invasion abilities. N=3. *p<0.05, **p<0.01, ***p<0.001. Scale bars: 50 μm.

with those in the PDCD10-overexpressing group, the viability of the cells in the PDCD10 + LY294002 group was significantly lower ($p<0.05$, Fig. 7A-D). Therefore, inhibiting the PI3K/AKT pathway can partly eliminate the radioresistance of EC cells with PDCD10 overexpression.

Discussion

PDCDs are a gene family related to programmed cell death, and several members have been well studied in relation to cancer development (Ghafouri-Fard et al., 2022). The differential expression of PDCDs can directly contribute to tumor progression. For example, *PDCD1* (Kannan et al., 2021), *PDCD2* (Mu et al., 2010), and *PDCD6* (Hu et al., 2019) are highly expressed in EC, where they promote the proliferation of tumor cells and are associated with a poor prognosis. Both *PDCD4* (Yang et al., 2014) and *PDCD5* (Xiao et al., 2023) are tumor suppressor genes involved in apoptosis and the cell cycle. In EC, dysregulation of their expression promotes the malignant progression of tumors; *PDCD7* has been identified as a direct target of miR-134 in oral squamous cell carcinoma (OSCC), reducing the expression of E-cadherin (E-cad), thereby promoting the oncogenicity of OSCC cells (Peng et al., 2018). PDCD10 plays an oncogenic role in PDAC (Zhou et al., 2024). Here, we found that the level of PDCD10 is elevated in patients with EC, contributing to the malignant progression of EC. Moreover, high expression of PDCD10 is a marker of a poor survival rate in patients with EC. Therefore, we believe that PDCD10 is a potential therapeutic approach and a prognostic biomarker for patients with EC.

It has been reported that PI3K/AKT is overexpressed in EC and is abnormally activated by various oncogenes or proteins (Luo et al., 2022). In this pathway, the activation of PI3K can promote the phosphorylation of AKT, thereby promoting cell growth and proliferation and inhibiting apoptosis (Shi et al., 2019a). Moreover, PI3K/AKT can increase the level of vascular endothelial growth factor (VEGF), promote angiogenesis in EC, and thus promote tumor growth and metastasis (Jiang and Liu, 2009). Moreover, the PI3K/AKT pathway can induce EMT, thus enhancing the migration and invasion abilities of EC cells (Li et al., 2017). In the treatment process, the activation of PI3K/AKT can also lead to chemoradiotherapy resistance in cancer cells, increasing the difficulty of treatment (Shi et al., 2019b; Zou et al., 2021). In response to these findings, researchers have used specific inhibitors of PI3K/AKT to inhibit the proliferation of EC cells and promote apoptosis in a

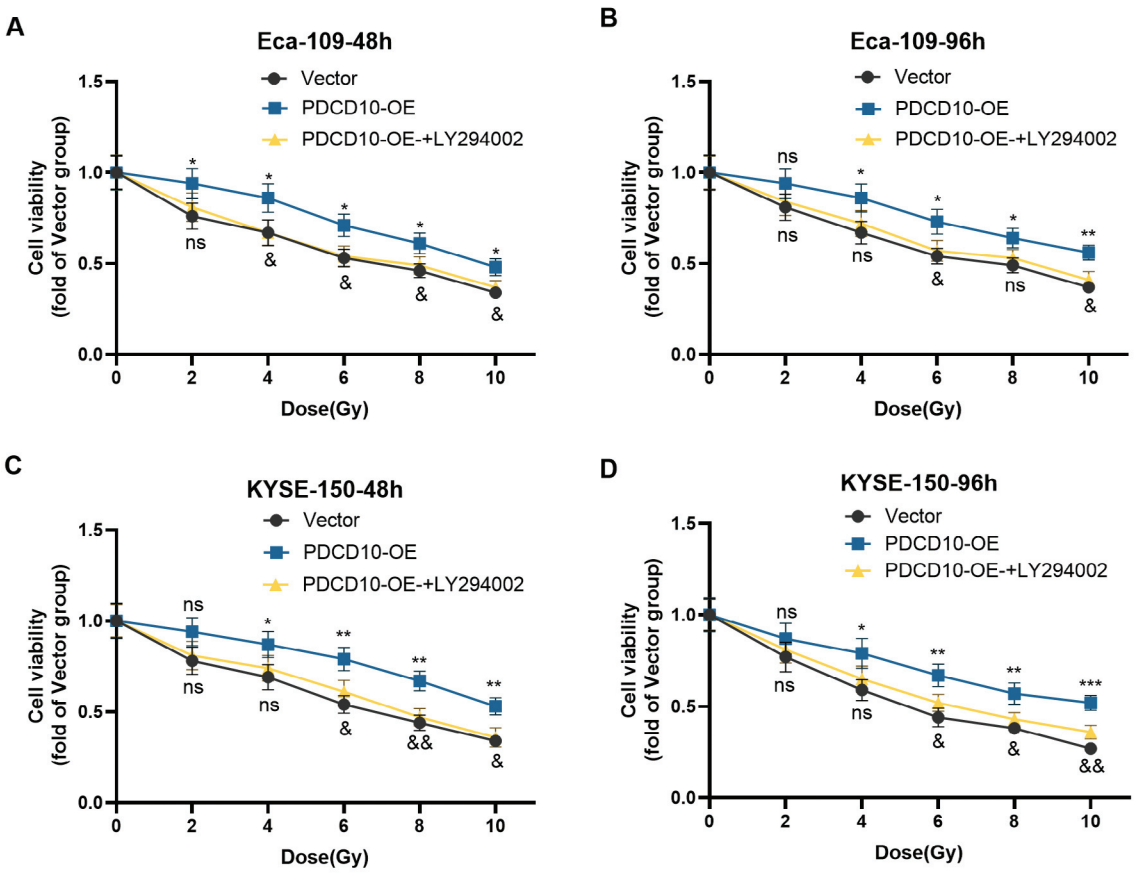

Fig. 7. Effects of PI3K inhibition on PDCD10-mediated radioresistance. Eca-109 cells overexpressing PDCD10 and treated with the PI3K inhibitor LY294002 (0.2 μM) were exposed to ionizing radiation (0, 2, 4, 6, 8, or 10 Gy). A CCK8 assay was performed at 48 and 96h to evaluate the survival rate of the tumor cells. ns, $p>0.05$, $^{*}p<0.05$, $^{**}p<0.01$, $^{***}p<0.001$ *vs.* the vector group; ns: not significant, $p>0.05$, $^{\&}p<0.05$, $^{\&\&}p<0.01$ vs. the PDCD10-OE group.

dose-dependent manner, which indicates the therapeutic potential of targeting PI3K/AKT in the treatment of EC (Li et al., 2014). Some studies have shown that PDCD10 enhances PI3K activity by interacting with VEGFR2, thus promoting the production of phosphatidylinositol-3,4,5-trisphosphate (PIP3). The C-terminal domain of PDCD10 binds to PIP3, further helping AKT localize to the cell membrane and promoting the phosphorylation of AKT. Therefore, PDCD10 can abnormally activate the PI3K/AKT signaling pathway and affect tumor progression (Dibble et al., 2010). To further verify this conclusion, we found that the expression of PI3K/AKT significantly decreased when PDCD10 was knocked down and that the expression of PI3K/AKT significantly increased when PDCD10 was overexpressed. When PI3K is inhibited, it can partially eliminate the proliferation, migration, and invasion abilities of EC cells induced by PDCD10 overexpression. Therefore, we believe that PDCD10 can target the PI3K/AKT pathway and affect EC.

Radiotherapy, along with surgery and chemotherapy, is one of the three fundamental methods for treating tumors. In the treatment of EC, for tumors that can be surgically resected, esophagectomy can be performed, whereas for advanced or unresectable tumors, radiotherapy and chemotherapy can be carried out. However, the tumor control and overall survival rates of patients with EC after standard treatment remain poor (Zhang and Wu, 2017). The main reason is that patients are extremely prone to treatment-related acute toxicity during radiotherapy, resulting in adverse reactions, including treatment-related pneumonia, postoperative pulmonary complications, esophagitis, and pericarditis. This toxicity is caused by the biological effects of irradiating rapidly dividing cells in the body. Moreover, long-term toxic effects may occur in some slowly dividing cell tissues in the body after treatment (Liao et al., 2007). Moreover, when EC patients choose radiotherapy, the radiation-induced DNA damage response (DDR) can induce a resistant tumor microenvironment (TME) by producing active mediators, which help to suppress immune function and cause metastasis, invasion, and radiotherapy resistance in EC (Cao et al., 2021). These limitations present many challenges for treating ESCC.

The resistance of tumor cells to radiotherapy is one of the main causes of treatment failure and recurrence. In recent years, studies have shown that members of the PDCD family play important roles in the radiosensitivity of tumors. For example, in glioblastoma multiforme (GBM), upregulating PDCD4 can reverse radioresistance mediated by miR-96 (Guo et al., 2018). In NPC, targeting PDCD6 can increase cellular radiosensitivity (Zhang et al., 2017). The PI3K/AKT pathway, an important intracellular signaling pathway that regulates cell survival, growth, proliferation, metabolism, and migration, is often activated during cancer radioresistance. Activated PI3K/AKT enables tumor cells to resist radiotherapy-induced apoptosis, thus affecting the effect of radiotherapy (Chang et al, 2013). Moreover, it allows tumor cells to repair the DNA damage caused by radiotherapy, thereby reducing the lethality of radiotherapy (Glorieux et al., 2020). Our study revealed that the expression of PI3K/AKT decreased in ESCC cells with PDCD10 downregulation. After PI3K/AKT pathway inhibition, the sensitivity of PDCD10-overexpressing ESCC cells to IR increased. These results indicate that PDCD10 can affect the radiosensitivity of ESCC by regulating the PI3K/AKT pathway.

Although this study revealed the potential mechanism by which PDCD10 promotes tumor progression through regulating the PI3K/AKT pathway in ESCC, the specific mechanism by which PDCD10 regulates the PI3K/AKT pathway still needs further exploration. More animal experiments are needed to verify the effects of PDCD10 on the metastasis and radiosensitivity of ESCC. In addition, clinical samples are lacking, making it impossible to detect the differential expression of PDCD10 in ESCC and other types of EC and its correlation with the prognosis of patients by measuring the expression level of PDCD10.

Conclusion

In summary, this study revealed increased expression of PDCD10 in ESCC. PDCD10 promotes the progression of ESCC by affecting the proliferation, migration, invasion, growth, apoptosis, and radiotherapy sensitivity of tumor cells. Furthermore, PDCD10 activates the PI3K/AKT signaling pathway, thereby mediating carcinogenic effects. This study reveals a new mechanism of ESCC progression, providing new insights for targeted therapy for ESCC.

Author contributions. J X: Conceptualization, Methodology, Funding acquisition, Project administration, Resources, Visualization, Writing-review & editing; QC: Investigation, Writing-review & editing, experiments conduction; QG: Data curation and analysis, Writing-review & editing; All the authors have read and approved the final manuscript.
Funding. This study was supported by the Fujian Province Young and Middle-Aged Teachers Education Research Project (No. JAT200531).
Ethics approval. This study was approved by the Ethics Committee of the Affiliated Hospital of Putian University (Approval number: 20230814). All procedures adhered to the ethical standards stated in the Declaration of Helsinki.
Consent to Participate. Not applicable.
Data availability. The data can be obtained from the corresponding authors upon reasonable request.
Competing interests. The authors declare that they have no competing interests.

References

Cao Y., Gao A., Li X., Min H., He C., Sun X., Ding W. Q. and Zhou J. (2021). Elevated TAB182 enhances the radioresistance of esophageal squamous cell carcinoma through G2-M checkpoint

modulation. Cancer Med. 10, 3101-3112.

Chang L., Graham P.H., Hao J., Ni J., Bucci J., Cozzi P. J., Kearsley J.H. and Li Y. (2013). Acquisition of epithelial-mesenchymal transition and cancer stem cell phenotypes is associated with activation of the PI3K/Akt/mTOR pathway in prostate cancer radioresistance. Cell Death Dis. 4, e875.

Chen E., Huang J., Chen M., Wu J., Ouyang P., Wang X., Shi D., Liu Z., Zhu W., Sun H., Yang S., Zhang B., Deng W., Qiu H. and Xie F. (2023a). FLI1 regulates radiotherapy resistance in nasopharyngeal carcinoma through TIE1-mediated PI3K/AKT signaling pathway. J. Transl. Med. 21, 134.

Chen B., Wang B., Xu X., Chen X., Yi W., Xu S. and Wang J. (2023b). Upregulation of NUAK2: A novel prognostic marker in breast cancer. Histol. Histopathol. 38, 811-822.

Dibble C.F., Horst J.A., Malone M.H., Park K., Temple B., Cheeseman H., Barbaro J.R., Johnson G.L. and Bencharit S. (2010). Defining the functional domain of programmed cell death 10 through its interactions with phosphatidylinositol-3,4,5-trisphosphate. PLoS One 5, e11740.

Ediriweera M.K., Tennekoon, K.H. and Samarakoon S.R. (2019). Role of the PI3K/AKT/mTOR signaling pathway in ovarian cancer: Biological and therapeutic significance. Semin. Cancer Biol. 59, 147-160.

Farhood B., Khodamoradi E., Hoseini-Ghahfarokhi M., Motevaseli E., Mirtavoos-Mahyari H., Eleojo Musa A. and Najafi M. (2020). TGF-β in radiotherapy: Mechanisms of tumor resistance and normal tissues injury. Pharmacol. Res. 155, 104745.

Fattahi S., Amjadi-Moheb F., Tabaripour R., Ashrafi G.H. and Akhavan-Niaki H. (2020). PI3K/AKT/mTOR signaling in gastric cancer: Epigenetics and beyond. Life Sci. 262, 118513.

Franken N.A., Rodermond H.M., Stap J., Haveman J. and van Bree C. (2006). Clonogenic assay of cells *in vitro*. Nat. Protoc. 1, 2315-2319.

Gao L., Zhang R., Zhang W., Lan Y., Li X., Cai Q. and Liu J. (2024). Integrated bioinformatics analysis and experimental validation on malignant progression and immune cell infiltration of LTBP2 in gliomas. BMC Cancer 24, 1252.

Ghafouri-Fard S., Hussen B.M., Mohaqiq M., Shoorei H., Baniahmad A., Taheri M. and Jamali E. (2022). Interplay between Non-Coding RNAs and programmed cell death proteins. Front. Oncol. 12, 808475.

Glaviano A., Foo A.S.C., Lam H.Y., Yap K.C.H., Jacot W., Jones R.H., Eng H., Nair M.G., Makvandi P., Geoerger B., Kulke M.H., Baird R.D., Prabhu J.S., Carbone D., Pecoraro C., Teh D.B.L., Sethi G., Cavalieri V., Lin K.H., Javidi-Sharifi N.R., Toska E., Davids M.S., Brown J.R., Diana P., Stebbing J., Fruman D.A. and Kumar A.P. (2023). PI3K/AKT/mTOR signaling transduction pathway and targeted therapies in cancer. Mol. Cancer 22, 138.

Glorieux M., Dok R. and Nuyts S. (2020). The influence of PI3K inhibition on the radiotherapy response of head and neck cancer cells. Sci. Rep. 10, 16208.

Guo P., Yu Y., Tian Z., Lin Y., Qiu Y., Yao W. and Zhang L. (2018). Upregulation of miR-96 promotes radioresistance in glioblastoma cells via targeting PDCD4. Int. J. Oncol. 53, 1591-1600.

Hu S., Zang R., Wang Y., Liang Y., Mu J., Zhang Y. and Ma J. (2019). Highly expressed microRNA-124 inhibits migration and promotes apoptosis of esophageal cancer cells by degrading PDCD6. J. BUON 24, 805-812.

Jiang B.H. and Liu L.Z. (2009). PI3K/PTEN signaling in angiogenesis and tumorigenesis. Adv. Cancer Res. 102, 19-65.

Kannan S., O'Connor G.M. and Bakker E.Y. (2021). Molecular mechanisms of PD-1 and PD-L1 activity on a Pan-Cancer basis: A bioinformatic exploratory study. Int. J. Mol. Sci. 22, 5478.

Li B., Li J., Xu W.W., Guan X.Y., Qin Y.R., Zhang L.Y., Law S., Tsao S.W. and Cheung A.L. (2014). Suppression of esophageal tumor growth and chemoresistance by directly targeting the PI3K/AKT pathway. Oncotarget 5, 11576-11587.

Li B., Xu W.W., Lam A.K.Y., Wang Y., Hu H.F., Guan X.Y., Qin Y.R., Saremi N., Tsao S.W., He Q.Y. and Cheung A.L.M. (2017). Significance of PI3K/AKT signaling pathway in metastasis of esophageal squamous cell carcinoma and its potential as a target for anti-metastasis therapy. Oncotarget 8, 38755-38766.

Liao Z., Cox J.D. and Komaki R. (2007). Radiochemotherapy of esophageal cancer. J. Thorac. Oncol. 2, 553-568.

Liu R., Chen Y., Liu G., Li C., Song Y., Cao Z., Li W., Hu J., Lu C. and Liu Y. (2020). PI3K/AKT pathway as a key link modulates the multidrug resistance of cancers. Cell Death Dis. 11, 797.

Liu X., He H., Zhang F., Hu X., Bi F., Li K., Yu H., Zhao Y., Teng X., Li J., Wang L., Zhang Y., and Wu Q. (2022a). m6A methylated EphA2 and VEGFA through IGF2BP2/3 regulation promotes vasculogenic mimicry in colorectal cancer via PI3K/AKT and ERK1/2 signaling. Cell Death Dis. 13, 483.

Liu J., Zhao K., Wu S., Li C., You C., Wang J., Shu K. and Lei T. (2022b). The dual role of PDCD10 in cancers: A promising therapeutic target. Cancers 14, 5986.

Luo Q., Du R., Liu W., Huang G., Dong Z. and Li X. (2022). PI3K/Akt/mTOR signaling pathway: Role in esophageal squamous cell carcinoma, regulatory mechanisms and opportunities for targeted therapy. Front. Oncol. 12, 852383.

Lyu C., Vaddi P.K., Elshafae S., Pradeep A., Ma D. and Chen S. (2025). Unveiling RACK1: A key regulator of the PI3K/AKT pathway in prostate cancer development. Oncogene 44, 322-335.

Mahmood T. and Yang P.C. (2012). Western blot: Technique, theory, and trouble shooting. N. Am. J. Med. Sci. 4, 429-434.

Maren N.A., Duduit J.R., Huang D., Zhao F., Ranney T.G. and Liu W. (2023). Stepwise optimization of Real-Time RT-PCR analysis. Methods Mol. Biol. 2653, 317-332.

Miricescu D., Totan A., Stanescu-Spinu I.I., Badoiu S.C., Stefani C. and Greabu M. (2020). PI3K/AKT/mTOR signaling pathway in breast cancer: From molecular landscape to clinical aspects. Int. J. Mol. Sci. 22, 173.

Morgan E., Soerjomataram I., Rumgay H., Coleman H.G., Thrift A.P., Vignat J., Laversanne M., Ferlay J. and Arnold M. (2022). The global landscape of esophageal squamous cell carcinoma and esophageal adenocarcinoma incidence and mortality in 2020 and projections to 2040: New estimates from GLOBOCAN 2020. Gastroenterology 163, 649-658.e2.

Mu W., Munroe R.J., Barker A.K. and Schimenti J.C. (2010). PDCD2 is essential for inner cell mass development and embryonic stem cell maintenance. Dev. Biol. 347, 279-288.

Peng S.Y., Tu H.F., Yang C.C., Wu C.H., Liu C.J., Chang K.W. and Lin S.C. (2018). miR-134 targets PDCD7 to reduce E-cadherin expression and enhance oral cancer progression. Int. J. Cancer 143, 2892-2904.

Qi, L., Sun, M., Liu, W., Zhang, X., Yu, Y., Tian, Z., Ni, Z., Zheng R. and Li Y. (2024). Global esophageal cancer epidemiology in 2022 and predictions for 2050: A comprehensive analysis and projections based on GLOBOCAN data. Chin. Med. J. 137, 3108-3116.

Romani A.M.P. (2022). Cisplatin in cancer treatment. Biochem.

Pharmacol. 206, 115323.
Saxton R.A. and Sabatini D.M. (2017). mTOR signaling in growth, metabolism, and disease. Cell 169, 361-371.
Sherman B.T., Panzade G., Imamichi T. and Chang W. (2024). DAVID Ortholog: An integrative tool to enhance functional analysis through orthologs. Bioinformatics 40, btae615.
Shi N., Yu H., and Chen T. (2019a). Inhibition of esophageal cancer growth through the suppression of PI3K/AKT/mTOR signaling pathway. OncoTargets Ther. 12, 7637-7647.
Shi J.J., Xing H., Wang Y.X., Zhang X., Zhan Q.M., Geng M.Y., Ding J., and Meng L.H. (2019b). PI3Kα inhibitors sensitize esophageal squamous cell carcinoma to radiation by abrogating survival signals in tumor cells and tumor microenvironment. Cancer Lett. 459, 145-155.
Spangle J.M., Roberts T.M. and Zhao J.J. (2017). The emerging role of PI3K/AKT-mediated epigenetic regulation in cancer. Biochim. Biophys Acta Rev. Cancer 1868, 123-131.
Sun B., Zhong F.J., Xu C., Li Y.M., Zhao Y.R., Cao M.M. and Yang L.Y. (2021). Programmed cell death 10 promotes metastasis and epithelial-mesenchymal transition of hepatocellular carcinoma via PP2Ac-mediated YAP activation. Cell Death Dis. 12, 849.
Sung H., Ferlay J., Siegel R.L., Laversanne M., Soerjomataram I., Jemal A. and Bray F. (2021). Global cancer statistics 2020: GLOBOCAN estimates of incidence and mortality Worldwide for 36 Cancers in 185 Countries. CA Cancer J. Clin. 71, 209-249.
Tan P., Ye Y., He L., Xie J., Jing J., Ma G., Pan H., Han L., Han W. and Zhou Y. (2018). TRIM59 promotes breast cancer motility by suppressing p62-selective autophagic degradation of PDCD10. PLoS Biol. 16, e3000051.
Teng Y., Xing Y., Xue W., Hu Y., Li Z., Qian J. and Wang R. (2024). Raddeanin A promotes the apoptosis of gastric cancer in conjunction with autophagy inhibitor Hydroxychloroquine via MAPK signaling pathway. J. Tradit. Complement. Med. 15, 161-169.
Tong X., Jin M., Wang L., Zhang D., Yin Y. and Shen Q. (2024). Prognostic biomarkers for immunotherapy in esophageal cancer. Front. Immunol. 15, 1420399.
Valentino M., Dejana E. and Malinverno M. (2020). The multifaceted PDCD10/CCM3 gene. Genes Dis. 8, 798-813.
Wu Y., He S., Cao M., Teng Y., Li Q., Tan N., Wang J., Zuo T., Li T., Zheng Y., Xia C. and Chen W. (2024). Comparative analysis of cancer statistics in China and the United States in 2024. Chin. Med. J. 137, 3093-3100.
Xiao Z., Si M., Cao J., Chen X., Wang Z., Zhang T., Zhou Y., Li H., Dai J., Wang C., Chen L. and Xu J. (2023). Cancer-testis non-coding RNA LEF1-AS1 regulates the nuclear translocation of PDCD5 and suppresses its interaction with p53 signaling: a novel target for immunotherapy in esophageal squamous cell carcinoma. Carcinogenesis 44, 263-276.
Xu J.C., Chen T.Y., Liao L.T., Chen T., Li Q.L., Xu J.X., Hu J.W., Zhou P.H. and Zhang Y.Q. (2021a). NETO2 promotes esophageal cancer progression by inducing proliferation and metastasis via PI3K/AKT and ERK pathway. Int. J. Biol. Sci. 17, 259-270.
Xu R., Zhang Y., Li A., Ma Y., Cai W., Song L., Xie Y., Zhou S., Cao W. and Tang X. (2021b). LY 294002 enhances the chemosensitivity of liver cancer to oxaliplatin by blocking the PI3K/AKT/HIF 1α pathway. Mol. Med. Rep. 24, 508.
Yang M., Liu R., Li X., Liao J., Pu Y., Pan E., Yin L. and Wang Y. (2014). miRNA-183 suppresses apoptosis and promotes proliferation in esophageal cancer by targeting PDCD4. Mol. Cells 37, 873-880.
Yang W., Cheng B., Chen P., Sun X., Wen Z. and Cheng Y. (2022). BTN3A1 promotes tumor progression and radiation resistance in esophageal squamous cell carcinoma by regulating ULK1-mediated autophagy. Cell Death Dis. 13, 984.
Yueyang M., Yaqin H., Guolian X., Wenjian Z., Yang J., Chen L., Haiyan C., Min C., Jianping D., Penggao D., Hongli Z. and Liang W. (2023). Glioma angiogenesis is boosted by ELK3 activating the HIF-1 α /VEGF-A signaling axis. BMC Cancer 23, 662.
Zhang M. and Wu A.J. (2017). Radiation techniques for esophageal cancer. Chin. Clin. Oncol. 6, 45.
Zhang Y., Zheng L., Lin S., Liu Y., Wang Y. and Gao F. (2017). MiR-124 enhances cell radiosensitivity by targeting PDCD6 in nasopharyngeal carcinoma. Int. J. Clin. Exp. Pathol. 10, 11461-11470.
Zhang Y., Zhang Y., Peng L. and Zhang L. (2022). Research progress on the predicting factors and coping strategies for postoperative recurrence of esophageal cancer. Cells 12, 114.
Zhang W., Xu Q., Shi C., Chen X., Shen C., Zhang Y., Zheng B. and Zhu H. (2024). RNA-binding protein DND1 participates in migration, invasion, and EMT of prostate cancer cells by degrading CLIC4. Histol. Histopathol. 39, 1343-1358.
Zhao Y.X., Zhao H.P., Zhao M.Y., Yu Y., Qi X., Wang J.H. and Lv J. (2024). Latest insights into the global epidemiological features, screening, early diagnosis and prognosis prediction of esophageal squamous cell carcinoma. World J. Gastroenterol. 30, 2638-2656.
Zhou Q., Breitkopf-Heinlein K., Gaitantzi H., Birgin E., Reissfelder C. and Rahbari N.N. (2024). PDCD10 promotes the tumor-supporting functions of TGF-β in pancreatic cancer. Clin. Sci. 138, 1111-1129.
Zou N., Zhang X., Li S., Li Y., Zhao Y., Yang X. and Zhu S. (2021). Elevated HNF1A expression promotes radiation-resistance via driving PI3K/AKT signaling pathway in esophageal squamous cell carcinoma cells. J. Cancer 12, 5013-5024.

Accepted October 29, 2025